

A structure-preserving parametric finite element method for area-conserved generalized mean curvature flow

Lifang Pei · Yifei Li

Received: date / Accepted: date

Abstract We propose and analyze a structure-preserving parametric finite element method (SP-PFEM) to simulate the motion of closed curves governed by area-conserved generalized mean curvature flow in two dimensions (2D). We first present a variational formulation and rigorously prove that it preserves two fundamental geometric structures of the flows, i.e., (a) the conservation of the area enclosed by the closed curve; (b) the decrease of the perimeter of the curve. Then the variational formulation is approximated by using piecewise linear parametric finite elements in space to develop the semi-discrete scheme. With the help of the discrete Cauchy's inequality and discrete power mean inequality, the area conservation and perimeter decrease properties of the semi-discrete scheme are shown. On this basis, by combining the backward Euler method in time and a proper approximation of the unit normal vector, a structure-preserving fully discrete scheme is constructed successfully, which can preserve the two essential geometric structures simultaneously at the discrete level. Finally, numerical experiments test the convergence rate, area conservation, perimeter decrease and mesh quality, and depict the evolution of curves. Numerical results indicate that the proposed SP-PFEM provides a reliable and powerful tool for the simulation of area-conserved generalized mean curvature flow in 2D.

Keywords area-conserved generalized mean curvature flow · parametric finite element method · area conservation · perimeter decrease

Mathematics Subject Classification (2020) 65M60 · 65M12 · 35K55 · 53C44

L. Pei
School of Mathematics and Statistics, Zhengzhou University, Zhengzhou, P. R. China 450001
E-mail: plf5801@zzu.edu.cn

Y. Li
Department of Mathematics, National University of Singapore, Singapore 119076
E-mail: e0444158@u.nus.edu

1 Introduction

Let $\Gamma(t)$ be a closed curve in two dimensions, which is represented by $\Gamma(t) = X(\cdot, t)$ with $X := X(s, t) = (x(s, t), y(s, t))^T \in \mathbb{R}^2$, where t denoting the time and s being the arc length parametrization of $\Gamma(t)$. The motion of $\Gamma(t)$ under the area-conserved generalized mean curvature flow is governed by the following geometric partial differential equation:

$$\begin{cases} \partial_t X = (\beta \kappa^\alpha - \lambda(t))n, & 0 < s < L(t), \quad t > 0, \\ \kappa = -\partial_{ss} X \cdot n, \end{cases} \quad (1.1)$$

where $L(t) := \int_{\Gamma(t)} 1 ds$ and $\kappa := \kappa(s, t)$ are the perimeter and the mean curvature of $\Gamma(t)$, respectively, $n := -(\partial_s X)^\perp$ is the outer unit normal to $\Gamma(t)$ with the notation $^\perp$ denoting clockwise rotation by $\frac{\pi}{2}$, α and β are real numbers satisfying $\alpha\beta < 0$, and

$$\lambda(t) = \frac{\int_{\Gamma(t)} \beta \kappa^\alpha ds}{L(t)} = \frac{\int_{\Gamma(t)} \beta \kappa^\alpha ds}{\int_{\Gamma(t)} 1 ds}, \quad (1.2)$$

which is specifically chosen such that the area enclosed by $\Gamma(t)$ is conserved. The initial data for (1.1) is given by

$$X(s, 0) = X_0(s) = (x_0(s), y_0(s))^T, \quad 0 \leq s \leq L(0), \quad (1.3)$$

where $L(0)$ is the perimeter of the initial curve $\Gamma(0) := \Gamma_0$.

Flows of the form (1.1) without the term $\lambda(t)$, which are called the generalized mean curvature flow, have been widely studied in the literature. For example, when $\alpha = 1$ and $\beta = -1$, this flow is the well-known mean curvature flow. It has been shown in [21, 23, 26] that the embedded curve evolving by the mean curvature flow shrinks to a point in finite time. Taking $0 < \alpha \neq 1$ and $\beta = -1$, we obtain the powers of mean curvature flow, which can be regarded as natural generalizations of the classical mean curvature flow (see [1, 39, 41–43]) and are fully nonlinear contracting flows for convex curves. In the case $\alpha = -1$ and $\beta = 1$, this flow is an expanding flow and coincides with the inverse mean curvature flow [1, 28, 29, 46], a weak notion of which was used to prove the Riemannian Penrose inequality. Urbas proved in [46] that the curve with the positive mean curvature $\kappa > 0$ stays strictly convex and smooth for all time, and exponentially converges, under appropriate rescaling, to a circle. This result can be extended to the case $\beta > 0$ and $-1 < \alpha < 0$ for infinite time or $\alpha < -1$ for finite time (see [1, 22, 34, 40]). However, all these contracting and expanding flows mentioned above have the property of some sort of singularity formation.

A tempting approach is to directly define a flow by adding a constraining term to prevent the singularity phenomenon. When the constraining term $\lambda(t)$ as (1.2) adopted, it can be shown that the flow (1.1) possess two fundamental geometric properties, i.e., (a) the area of the region enclosed by the curve is conserved; (b) the perimeter of the curve decreases in time. In this case, the initial curve governed by this flow exists for all times and converges smoothly to a round circle. For more details, we refer [2, 13, 16, 19, 20, 24, 27, 32, 36, 44, 45] and reference therein. Thus (1.1)–(1.2) can be interpreted as a unified flow model with fixed areas and perimeters

decrease properties, which has important applications in many research areas, such as material science and shape recovery in image processing [17].

In this paper, we will investigate numerical approximations of the area-conserved generalized mean curvature flow (1.1)–(1.2), paying particular attention to the two essential geometric structure preserving aspects. In the last decades, for the special case $\alpha = 1$ and $\beta = -1$, i.e., area-conserved mean curvature flow, there have been various numerical methods in the literature, e.g., the finite difference method [37], the level set method [38], MBO method [31] and crystalline algorithm [47]. However, among them, structure-preserving properties were barely investigated except for the crystalline algorithm in [47], which was shown to be area-preserving and perimeter decreasing. Since the crystalline algorithm involves the crystalline motion governed by a system of ordinary differential equations, it is no easy task to apply to the generalized model (1.1)–(1.2). Recently, a parametric finite element method (PFEM) was developed for the flow (1.1)–(1.2) with $\alpha = 1$ and $\beta = -1$ in [12]. The PFEM was presented by Barrett, Garcke and Nürnberg (BGN) first for surface diffusion flows in [10] based on ideas of Dziuk [18]. Different from the parametric methods in [3, 14, 15, 35], the PFEM involves an elegant variational formulation that allows tangential degrees of freedom so that the mesh quality can be improved significantly. Up to now, this method has been extensively applied to simulate geometric flows [5, 6, 8, 9, 11, 33, 48]. It is shown in [12] that the semi-discrete version of the PFEM leads to the equidistribution of mesh points along curves during the evolution, i.e., equal mesh distribution. This property prevents the possible mesh distortion and avoids the complex and undesired re-meshing steps, which plays a vital role in numerical simulations. Moreover, the PFEM in [12] enjoys unconditional perimeter decrease law. But the fully discrete scheme fails to exactly conserve the enclosed area of the discrete solution, which may lead to a challenge on the accuracy of the numerical solutions. In this situation, it is a natural requirement to develop novel numerical schemes that can inherit the good properties of the PFEM and preserve the enclosed area for the area-conserved generalized mean curvature flow (1.1)–(1.2).

Recently, for surface diffusion flow, which also has area-conservation and perimeter decrease properties, we notice that a structure-preserving fully discrete PFEM was introduced in [30] to preserve the two geometric properties for the discretized solutions. Nevertheless, the mesh quality is not well preserved during time evolution. Subsequently, motivated by the original ideas of [30] and BGN [10], Bao and Zhao constructed a structure-preserving PFEM in [7] for surface diffusion flow. The proposed method not only achieves the exact conservation of the enclosed area and decrease of perimeter, but also has asymptotic equal mesh distribution property, that is to say, mesh points on the polygonal curve tend to be equally distributed during the evolution and eventually be equidistributed. Very recently, by combining the skills from [7, 30] and axisymmetric variational discretizations, a structure-preserving PFEM was developed in [4] for axisymmetric geometric evolution equations.

Inspired by [7, 30], we try to propose a structure-preserving PFEM (SP-PFEM) for the area-conserved generalized mean curvature flow (1.1)–(1.2) such that its two geometric structures are well preserved. We need to deal with troubles and challenges brought by the nonlinear term κ^α and the nonlocal term $\lambda(t)$, and hope that the SP-PFEM are available for all cases of α . We first present a variational

formulation and show the area conservation and perimeter decrease properties by utilizing Cauchy's inequality and the power mean inequality. Then we discretize the variational formulation with the PFEM in space, and prove rigorously that the semi-discrete scheme preserves the two geometric structures with the help of the discrete Cauchy's inequality and discrete power mean inequality. On this basis, by transferring the novel approach in [7] to the approximation of the flow (1.1)–(1.2), we choose the backward Euler method in time and a proper approximation of the unit normal vector combining the information of the curves at the current and next time step to construct a fully discrete scheme. It can be shown that the proposed scheme is area preserving and unconditional perimeter decreasing. Numerical experiments reveal that it also enjoys asymptotic equal mesh distribution property. The main contribution of our work lies in: (I) we establish a unified structure-preserving PFEM for the area-conserved generalized mean curvature flow, which is accurate and efficient in practical simulations; (II) the area conservation and perimeter decrease properties are rigorously proved for variational formulation, semi-discrete scheme and fully discrete scheme.

The rest of the paper is organized as follows. In section 2, we investigate the two geometric structures properties of the variational formulation. In section 3, a PFEM semi-discrete scheme is developed, and its area conservation and perimeter dissipation properties are proved rigorously. In section 4, we propose a SP-PFEM fully-discrete scheme, provide the proof of its structure preserving property, and present iterative methods for solving the resulting nonlinear system. Furthermore, numerical results are reported in section 5 to demonstrate the accuracy and efficiency of the proposed SP-PFEM, and some conclusions are drawn in section 6.

2 The variational formulation and its properties

In this section, we present a variational formulation for the area-conserved generalized mean curvature flow (1.1)–(1.2) and establish its area conservation and perimeter decrease properties.

To obtain the variational formulation, a time independent variable ρ is introduced such that $\Gamma(t)$ can be parameterized over the fixed domain $\rho \in \mathbb{I} = \mathbb{R}/\mathbb{Z} = [0, 1]$ as

$$\Gamma(t) := X(\cdot, t), \quad X(\cdot, t) : \mathbb{I} \rightarrow \mathbb{R}^2, \quad (\rho, t) \mapsto X(\rho, t) = (x(\rho, t), y(\rho, t))^T. \quad (2.1)$$

Based on this parametrization, the arc length parameter s is computed by $s(\rho, t) = \int_0^\rho |\partial_q X| dq$, and there holds $\partial_\rho s = |\partial_\rho X|$, $ds = \partial_\rho s d\rho = |\partial_\rho X| d\rho$. During the evolution, we assume that the mean curvature $\kappa(\cdot, t)$ of $\Gamma(t)$ satisfies

$$\kappa(\cdot, t) \geq 0 \quad \forall 0 < \alpha \neq 1 \quad \text{and} \quad \kappa(\cdot, t) > 0 \quad \forall \alpha < 0, \quad \forall t \geq 0. \quad (2.2)$$

Besides, we further assume that during the evolution, there is a constant $C > 1$ such that $1/C \leq |\partial_\rho X| \leq C$, i.e., $\Gamma(t)$ is regular for all t .

As a preparation, we define the functional space as

$$L_p^2(\mathbb{I}) = \left\{ u : \mathbb{I} \rightarrow \mathbb{R} \mid \int_{\mathbb{I}} |u(\rho)|^2 d\rho < +\infty \right\} \quad (2.3)$$

equipped with the weighted L^2 -inner product with respect to the closed curve $\Gamma(t)$

$$(u, v)_{\Gamma(t)} := \int_{\Gamma(t)} u(s)v(s)ds = \int_{\mathbb{I}} u(s(\rho, t))v(s(\rho, t))\partial_\rho s d\rho, \quad \forall u, v \in L_p^2(\mathbb{I}). \quad (2.4)$$

We note that the assumption $1/C \leq |\partial_\rho X| \leq C$ ensures the weighted inner products with respect to different $\Gamma(t)$ s are equivalent, and thus the $L_p^2(\mathbb{I})$ can be interpreted as the usual $L_p^2(\mathbb{I})$ space.

At the same time, we introduce the Sobolev space

$$H_p^1(\mathbb{I}) = \left\{ u : \mathbb{I} \rightarrow \mathbb{R} \mid u \in L_p^2(\mathbb{I}), \partial_\rho u \in L_p^2(\mathbb{I}) \right\}.$$

These notations can be easily extended to $[L_p^2(\mathbb{I})]^2$ and $[H_p^1(\mathbb{I})]^2$ for vector-valued functions.

By applying the identity $\kappa n = -\partial_{ss}X$ given in [18], we reformulate (1.1) into

$$\partial_t X \cdot n = \beta \kappa^\alpha - \lambda(t), \quad 0 < s < L(t), \quad t > 0, \quad (2.5a)$$

$$\kappa n = -\partial_{ss}X. \quad (2.5b)$$

Then by taking the L^2 -inner product of (2.5a) with a test function $\phi \in H_p^1(\mathbb{I})$, we have

$$(\partial_t X \cdot n, \phi)_{\Gamma(t)} - (\beta \kappa^\alpha - \lambda(t), \phi)_{\Gamma(t)} = 0. \quad (2.6)$$

Similarly, take the L^2 -inner product of (2.5b) with a test function $\omega = (\omega_1, \omega_2)^T \in [H_p^1(\mathbb{I})]^2$ and integrating by parts, we get

$$(\kappa n, \omega)_{\Gamma(t)} - (\partial_s X, \partial_s \omega)_{\Gamma(t)} = 0. \quad (2.7)$$

Therefore, the variational formulation of (1.1)–(1.2) with the initial condition (1.3) can be stated as follows: Given the initial curve $\Gamma(0) := \Gamma_0$ with $X(\cdot, 0) \in [H_p^1(\mathbb{I})]^2$, find the curve $\Gamma(t) := X(\cdot, t) = (x(\cdot, t), y(\cdot, t))^T \in [H_p^1(\mathbb{I})]^2$ and the mean curvature $\kappa(\cdot, t) \in H_p^1(\mathbb{I})$ such that

$$\begin{cases} (\partial_t X \cdot n, \phi)_{\Gamma(t)} - (\beta \kappa^\alpha - \lambda(t), \phi)_{\Gamma(t)} = 0, & \phi \in H_p^1(\mathbb{I}), \\ (\kappa n, \omega)_{\Gamma(t)} - (\partial_s X, \partial_s \omega)_{\Gamma(t)} = 0, & \omega \in [H_p^1(\mathbb{I})]^2. \end{cases} \quad (2.8)$$

Let $\Omega(t)$ be the region enclosed by the curve $\Gamma(t)$ and

$$A(t) := \int_{\Omega(t)} dx dy = \int_0^{L(t)} y(s, t) \partial_s x(s, t) ds, \quad t \geq 0 \quad (2.9)$$

be the area of $\Omega(t)$. Then we have

Theorem 1 (Area conservation and perimeter decrease)

Let $(X(\cdot, t), \kappa(\cdot, t)) \in [H_p^1(\mathbb{I})]^2 \times H_p^1(\mathbb{I})$ be a solution of the variational formulation (2.8) with the assumption (2.2) holds on $\kappa(\cdot, t)$. Then the area $A(t)$ is conserved and the perimeter $L(t)$ is decreasing, i.e., $\forall t \geq t_1 \geq 0$, there holds

$$A(t) = A(t_1) \equiv A(0) := \int_0^{L(0)} y_0(s) \partial_s x_0(s) ds, \quad L(t) \leq L(t_1) \leq L(0). \quad (2.10)$$

Proof Differentiating $A(t)$ with respect to t and integrating by parts, we obtain

$$\begin{aligned}
\frac{dA(t)}{dt} &= \frac{d}{dt} \int_0^{L(t)} y(s,t) \partial_s x(s,t) ds = \frac{d}{dt} \int_0^1 y(\rho,t) \partial_\rho x(\rho,t) d\rho \\
&= \int_0^1 (\partial_t y \partial_\rho x + y \partial_t \partial_\rho x) d\rho = \int_0^1 (\partial_t y \partial_\rho x - \partial_\rho y \partial_t x) d\rho + (y \partial_t x)|_{\rho=0}^{\rho=1} \\
&= \int_0^1 (\partial_t X) \cdot (-\partial_\rho y, \partial_\rho x) d\rho = (\partial_t X \cdot n, 1)_{\Gamma(t)} = (\beta \kappa^\alpha - \lambda(t), 1)_{\Gamma(t)} \\
&= \beta \int_{\Gamma(t)} \kappa^\alpha ds - \beta \frac{\int_{\Gamma(t)} \kappa^\alpha ds}{L(t)} \int_{\Gamma(t)} 1 ds \equiv 0,
\end{aligned} \tag{2.11}$$

where we used the first equation in (2.8) by taking $\phi \equiv 1$. Obviously, formula (2.11) immediately implies the area-preserving property in (2.10).

Similarly, differentiating $L(t)$ with respect to t and integrating by parts, we have

$$\begin{aligned}
\frac{dL(t)}{dt} &= \frac{d}{dt} \int_0^{L(t)} 1 ds = \frac{d}{dt} \int_0^1 \partial_\rho s d\rho = \frac{d}{dt} \int_0^1 |\partial_\rho X| d\rho \\
&= \int_0^1 \frac{\partial_\rho X \cdot (\partial_\rho \partial_t X)}{|\partial_\rho X|} d\rho = \int_0^1 \partial_\rho X \partial_s \rho \cdot (\partial_s \partial_t X) \partial_\rho s d\rho \\
&= \int_{\Gamma(t)} \partial_s X \cdot (\partial_s \partial_t X) ds = (\partial_s X, \partial_s \partial_t X)_{\Gamma(t)}.
\end{aligned} \tag{2.12}$$

Setting $\omega = \partial_t X$ and $\phi = \kappa$ in the variational formulation (2.8), we get

$$\begin{aligned}
\frac{dL(t)}{dt} &= (\kappa n, \partial_t X)_{\Gamma(t)} = (\partial_t X \cdot n, \kappa)_{\Gamma(t)} = (\beta \kappa^\alpha - \lambda(t), \kappa)_{\Gamma(t)} \\
&= L(t) \beta \left[\frac{1}{L(t)} \int_{\Gamma(t)} \kappa^{\alpha+1} ds - \frac{1}{L(t)^2} \left(\int_{\Gamma(t)} \kappa^\alpha ds \right) \left(\int_{\Gamma(t)} \kappa ds \right) \right].
\end{aligned} \tag{2.13}$$

When $\alpha = 1$ and $\beta < 0$, for any $\kappa \in \mathbb{R}$, by Cauchy's inequality, we have

$$\left(\int_{\Gamma(t)} \kappa ds \right)^2 \leq \int_{\Gamma(t)} 1 ds \int_{\Gamma(t)} \kappa^2 ds, \tag{2.14}$$

thus

$$\begin{aligned}
\frac{dL(t)}{dt} &= L(t) \beta \left[\frac{1}{L(t)} \int_{\Gamma(t)} \kappa^2 ds - \frac{1}{L(t)^2} \left(\int_{\Gamma(t)} \kappa ds \right) \left(\int_{\Gamma(t)} \kappa ds \right) \right] \\
&\leq L(t) \beta \left[\frac{1}{L(t)} \int_{\Gamma(t)} \kappa^2 ds - \frac{1}{L(t)^2} \left(\int_{\Gamma(t)} 1 ds \right) \left(\int_{\Gamma(t)} \kappa^2 ds \right) \right] = 0.
\end{aligned} \tag{2.15}$$

When $\alpha = -1$, $\kappa > 0$ and $\beta > 0$, by Cauchy's inequality, we have

$$\left(\int_{\Gamma(t)} 1 ds \right)^2 \leq \int_{\Gamma(t)} \frac{1}{\kappa} ds \int_{\Gamma(t)} \kappa ds, \tag{2.16}$$

which combines with $\beta > 0$ also implies

$$\frac{dL(t)}{dt} = L(t) \beta \left[\frac{1}{L(t)} \int_{\Gamma(t)} 1 ds - \frac{1}{L(t)^2} \left(\int_{\Gamma(t)} \frac{1}{\kappa} ds \right) \left(\int_{\Gamma(t)} \kappa ds \right) \right] \leq 0. \tag{2.17}$$

Therefore the perimeter decrease property in (2.10) holds for $|\alpha| = 1$.

When $0 < |\alpha| \neq 1$, to show $\frac{dL(t)}{dt} \leq 0$, we need the power mean inequality [25][Page 144]:

Lemma 1 (Power mean inequality) *For any finite interval $E = (a, b)$, and the non-zero parameters p, q satisfy $-\infty < p < q < \infty$. Suppose $f(x)$ is bounded and $f \geq 0$ in E if $p > 0$, and $f > 0$ in E if $p < 0$, we have*

$$\left(\frac{\int_a^b f^p(x) dx}{|b-a|} \right)^{\frac{1}{p}} \leq \left(\frac{\int_a^b f^q(x) dx}{|b-a|} \right)^{\frac{1}{q}}. \quad (2.18)$$

For the case $\alpha > 0, \alpha \neq 1$ and $\kappa \geq 0$, we know $\beta < 0$. By taking $E := \Gamma(t)$, $(f, p, q) = (\kappa^\alpha, 1, \frac{\alpha+1}{\alpha})$ and $(\kappa, 1, \alpha+1)$, respectively, we obtain

$$\frac{\int_{\Gamma(t)} \kappa^\alpha ds}{L(t)} \leq \left(\frac{\int_{\Gamma(t)} \kappa^{\alpha+1} ds}{L(t)} \right)^{\frac{\alpha}{\alpha+1}}, \quad \frac{\int_{\Gamma(t)} \kappa ds}{L(t)} \leq \left(\frac{\int_{\Gamma(t)} \kappa^{\alpha+1} ds}{L(t)} \right)^{\frac{1}{\alpha+1}}. \quad (2.19)$$

By substituting (2.19) in (2.13), we have

$$\begin{aligned} \frac{dL(t)}{dt} = L(t)\beta & \left[\left(\frac{\int_{\Gamma(t)} \kappa^{\alpha+1} ds}{L(t)} \right)^{\frac{\alpha}{\alpha+1}} \left(\frac{\int_{\Gamma(t)} \kappa^{\alpha+1} ds}{L(t)} \right)^{\frac{1}{\alpha+1}} \right. \\ & \left. - \frac{1}{L(t)^2} \left(\int_{\Gamma(t)} \kappa^\alpha ds \right) \left(\int_{\Gamma(t)} \kappa ds \right) \right] \leq 0. \end{aligned} \quad (2.20)$$

For the case $\alpha < 0, \alpha \neq -1$ and $\kappa > 0$, we know $\beta > 0$. By taking $E := \Gamma(t)$, $(f, p, q) = (\kappa^\alpha, \frac{\alpha+1}{\alpha}, 1)$ and $(\kappa, \alpha+1, 1)$, respectively, we obtain

$$\left(\frac{\int_{\Gamma(t)} \kappa^{\alpha+1} ds}{L(t)} \right)^{\frac{\alpha}{\alpha+1}} \leq \frac{\int_{\Gamma(t)} \kappa^\alpha ds}{L(t)}, \quad \left(\frac{\int_{\Gamma(t)} \kappa^{\alpha+1} ds}{L(t)} \right)^{\frac{1}{\alpha+1}} \leq \frac{\int_{\Gamma(t)} \kappa ds}{L(t)}. \quad (2.21)$$

Similarly, by substituting (2.21) in (2.13), we have $\frac{dL(t)}{dt} \leq 0$. Thus, the perimeter decrease property in (2.10) is proven for all possible α cases. The proof is completed.

3 A PFEM semi-discrete scheme and its properties

In this section, we present a parametric finite element method (PFEM) with conforming piecewise linear elements to discretize the variational formulation (2.8) in space direction, and show that the scheme preserves the area conservation and perimeter decrease properties.

3.1 The semi-discretization in space

Assume that the interval \mathbb{I} is divided into a uniform partition $\mathbb{I} = \bigcup_{j=1}^N I_j$ with the grid points $\{\rho_j := jh\}_{j=0}^N$, where $\rho_0 = \rho_N$ by periodic, the subintervals $I_j = [\rho_{j-1}, \rho_j]$ for $j = 1, 2, \dots, N$, $N \geq 3$ is a positive integer and $h = 1/N$. Let $\mathcal{P}_1(I_j)$ be the space of all polynomials with degree at most 1 over I_j , then the conforming linear finite element space can be described by

$$\mathbb{V}^h := \left\{ u^h \in C(\mathbb{I}) \mid u^h|_{I_j} \in \mathcal{P}_1(I_j), \quad \forall j = 1, 2, \dots, N \right\}.$$

Let $\Gamma^h(t) := X^h(\cdot, t) = (x^h(\cdot, t), y^h(\cdot, t))^T \in [\mathbb{V}^h]^2$ and $\kappa^h(\cdot, t) \in \mathbb{V}^h$ be the piecewise linear finite element approximation of the solution $(X(\cdot, t), \kappa(\cdot, t)) \in [H_p^1(\mathbb{I})]^2 \times H_p^1(\mathbb{I})$ of the variational formulation (2.8). In fact, the polygonal curve $\Gamma^h(t)$ consists of ordered line segments $\{h_j\}_{j=1}^N$, and we always assume that they satisfy

$$h_{\min}(t) := \min_{1 \leq j \leq N} |h_j(t)| > 0 \quad \text{with} \quad h_j(t) := X^h(\rho_j, t) - X^h(\rho_{j-1}, t), \quad (3.1)$$

where $|h_j(t)|$ denotes the length of the vector $h_j(t)$. Similar to the continuous equation, we further propose the following assumption on $\kappa^h(\cdot, t)$:

$$\kappa^h(\rho_j, t) \geq 0 \quad \forall 0 < \alpha \neq 1 \quad \text{and} \quad \kappa^h(\rho_j, t) > 0 \quad \forall \alpha < 0, \quad \forall j = 0, 1, \dots, N, \quad t \geq 0. \quad (3.2)$$

Meanwhile, it is easy to check that the unit tangential vector τ^h and the outward unit normal vector n^h of the curve $\Gamma^h(t)$ are constant vectors on each interval I_j . They can be computed on each interval I_j as

$$\tau^h|_{I_j} = \frac{h_j}{|h_j|} := \tau_j^h, \quad n^h|_{I_j} = -(\tau_j^h)^\perp = -\frac{(h_j)^\perp}{|h_j|} := n_j^h, \quad \forall j = 1, 2, \dots, N. \quad (3.3)$$

Furthermore, for two piecewise continuous scalar/vector functions u and v defined on \mathbb{I} , with possible jumps at the nodes $\{\rho_j\}_{j=0}^N$, we introduce the mass lumped inner product $(\cdot, \cdot)_{\Gamma^h(t)}^h$ over $\Gamma^h(t)$ as

$$(u, v)_{\Gamma^h}^h := \frac{1}{2} \sum_{j=1}^N |h_j| \left[(u \cdot v)(\rho_j^-) + (u \cdot v)(\rho_{j-1}^+) \right], \quad (3.4)$$

where $u(\rho_j^\pm) = \lim_{\rho \rightarrow \rho_j^\pm} u(\rho)$ for $j = 0, 1, \dots, N$ are the one-sided limits.

Then a semi-discrete scheme based on the variational formulation (2.8) can be constructed as: Given the initial curve $\Gamma^h(0) := \Gamma_0^h$ with $X^h(\cdot, 0) \in [\mathbb{V}^h]^2$, find the closed curve $\Gamma^h(t) := X^h(\cdot, t) = (x^h(\cdot, t), y^h(\cdot, t))^T \in [\mathbb{V}^h]^2$ and the mean curvature $\kappa^h(\cdot, t) \in \mathbb{V}^h$ such that

$$\begin{cases} (\partial_t X^h \cdot n^h, \phi^h)_{\Gamma^h}^h - (\beta(\kappa^h)\alpha - \lambda^h, \phi^h)_{\Gamma^h}^h = 0, & \phi^h \in \mathbb{V}^h, \\ (\kappa^h n^h, \omega^h)_{\Gamma^h}^h - (\partial_s X^h, \partial_s \omega^h)_{\Gamma^h}^h = 0, & \omega^h \in [\mathbb{V}^h]^2, \end{cases} \quad (3.5)$$

where $\Gamma^h(0) = X^h(\cdot, 0) \in [\mathbb{V}^h]^2$ is the interpolation of the initial curve Γ_0 satisfying $X^h(\rho_j, 0) = X(\rho_j, 0), \forall j = 0, 1, 2, \dots, N$, and

$$\lambda^h = \frac{(\beta(\kappa^h)^\alpha, 1)_{\Gamma^h}^h}{(1, 1)_{\Gamma^h}^h}. \quad (3.6)$$

3.2 Area conservation and perimeter decrease

Denote the area of the region enclosed by the closed curve $\Gamma^h(t)$ by $A^h(t)$ and the perimeter of $\Gamma^h(t)$ by $L^h(t)$, which are defined as follows:

$$A^h(t) := \frac{1}{2} \sum_{j=1}^N (x_j - x_{j-1})(y_j + y_{j-1}), \quad L^h(t) := \sum_{j=1}^N |h_j(t)| = (1, 1)_{\Gamma^h}^h, \quad (3.7)$$

where $X_j(t) = (x_j(t), y_j(t))^T := X^h(\rho_j, t)$ for $j = 0, 1, \dots, N$. Then we have

Theorem 2 (Area conservation and perimeter decrease)

Let $(X^h(\cdot, t), \kappa^h(\cdot, t)) \in [\mathbb{V}^h]^2 \times \mathbb{V}^h$ be a solution of the PFEM semi-discrete scheme (3.5) with the assumption (3.2) holds on $\kappa^h(\cdot, t)$. Then the area $A^h(t)$ is conserved and the perimeter $L^h(t)$ is decreasing, i.e., for $t \geq t_1 \geq 0$, there holds

$$A^h(t) = A^h(t_1) \equiv A^h(0) := \frac{1}{2} \sum_{j=1}^N [x_0(s_j) - x_0(s_{j-1})] [y_0(s_j) + y_0(s_{j-1})], \quad (3.8)$$

$$L^h(t) \leq L^h(t_1) \leq L^h(0) := \sum_{j=1}^N |h_j(0)|. \quad (3.9)$$

Proof By applying proposition 3.1 in [48], we obtain

$$\frac{dA^h(t)}{dt} = \frac{1}{2} \sum_{j=1}^N (\partial_t X_j^h + \partial_t X_{j-1}^h) \cdot (|h_j| n_j^h) = (\partial_t X^h \cdot n^h, 1)_{\Gamma^h}^h. \quad (3.10)$$

Taking $\phi^h \equiv 1$ in (3.5), and employing (3.6) and (3.10), we are able to derive

$$\frac{dA^h(t)}{dt} = \left(\beta(\kappa^h)^\alpha - \lambda^h, 1 \right)_{\Gamma^h}^h = \left(\beta(\kappa^h)^\alpha, 1 \right)_{\Gamma^h}^h - \frac{(\beta(\kappa^h)^\alpha, 1)_{\Gamma^h}^h}{(1, 1)_{\Gamma^h}^h} (1, 1)_{\Gamma^h}^h \equiv 0, \quad (3.11)$$

which leads to (3.8) immediately. In other words, $A^h(t)$ is conserved.

At the same time, differentiating $L^h(t)$ with respect to t , we get

$$\begin{aligned} \frac{dL^h(t)}{dt} &= \frac{d}{dt} \left(\sum_{j=1}^N |h_j| \right) = \sum_{j=1}^N \frac{h_j}{|h_j|} \cdot \frac{dh_j}{dt} = \sum_{j=1}^N |h_j| \tau_j^h \cdot \frac{1}{|h_j|} \frac{dh_j}{dt} \\ &= \sum_{j=1}^N |h_j| (\partial_s X^h) |_{I_j} \cdot (\partial_s (\partial_t X^h)) |_{I_j} = (\partial_s X^h, \partial_s \partial_t X^h)_{\Gamma^h}^h. \end{aligned} \quad (3.12)$$

Taking $\phi^h = \kappa^h$ and $\omega^h = \partial_t X^h$ in (3.5), combining (3.6) and (3.12), we can deduce that

$$\begin{aligned} \frac{dL^h(t)}{dt} &= \left(\kappa^h n^h, \partial_t X^h \right)_{\Gamma^h}^h = \left(\beta (\kappa^h)^\alpha - \lambda^h, \kappa^h \right)_{\Gamma^h}^h \\ &= \beta \left[\left((\kappa^h)^\alpha, \kappa^h \right)_{\Gamma^h}^h - \frac{\left((\kappa^h)^\alpha, 1 \right)_{\Gamma^h}^h \left(1, \kappa^h \right)_{\Gamma^h}^h}{\left(1, 1 \right)_{\Gamma^h}^h} \right]. \end{aligned} \quad (3.13)$$

When $|\alpha| = 1$, it follows from the Cauchy's inequality and the arithmetic-geometric/-harmonic mean inequality that

$$\begin{aligned} (\kappa^h, 1)_{\Gamma^h}^h (\kappa^h, 1)_{\Gamma^h}^h &= \left(\frac{1}{2} \sum_{j=1}^N |h_j| \left(\kappa^h(\rho_j^-) + \kappa^h(\rho_{j-1}^+) \right) \right)^2 \\ &\leq \left(\sum_{j=1}^N |h_j| \right) \left(\frac{1}{4} \sum_{j=1}^N |h_j| \left(\kappa^h(\rho_j^-) + \kappa^h(\rho_{j-1}^+) \right)^2 \right) \\ &\leq \left(\sum_{j=1}^N |h_j| \right) \left(\frac{1}{4} \sum_{j=1}^N |h_j| 2 \left((\kappa^h(\rho_j^-))^2 + (\kappa^h(\rho_{j-1}^+))^2 \right) \right) \\ &= (1, 1)_{\Gamma^h}^h (\kappa^h, \kappa^h)_{\Gamma^h}^h, \end{aligned} \quad (3.14)$$

and

$$\begin{aligned} (1, 1)_{\Gamma^h}^h \left((\kappa^h)^{-1}, \kappa^h \right)_{\Gamma^h}^h &= (1, 1)_{\Gamma^h}^h (1, 1)_{\Gamma^h}^h = \left(\sum_{j=1}^N |h_j| \right)^2 \\ &\leq \left(\sum_{j=1}^N |h_j| \frac{\frac{1}{\kappa^h(\rho_j^-)} + \frac{1}{\kappa^h(\rho_{j-1}^+)}}{2} \right) \left(\sum_{j=1}^N |h_j| \frac{2}{\frac{1}{\kappa^h(\rho_j^-)} + \frac{1}{\kappa^h(\rho_{j-1}^+)}} \right) \\ &\leq \left(\sum_{j=1}^N |h_j| \frac{\frac{1}{\kappa^h(\rho_j^-)} + \frac{1}{\kappa^h(\rho_{j-1}^+)}}{2} \right) \left(\sum_{j=1}^N |h_j| \frac{\kappa^h(\rho_j^-) + \kappa^h(\rho_{j-1}^+)}{2} \right) \\ &= \left((\kappa^h)^{-1}, 1 \right)_{\Gamma^h}^h (\kappa^h, 1)_{\Gamma^h}^h. \end{aligned} \quad (3.15)$$

Substituting (3.14)–(3.15) into (3.13) for $\alpha = \pm 1$, respectively, and using $\alpha\beta < 0$, we deduce that

$$\frac{dL^h(t)}{dt} = \beta \left[\left((\kappa^h)^\alpha, \kappa^h \right)_{\Gamma^h}^h - \frac{\left((\kappa^h)^\alpha, 1 \right)_{\Gamma^h}^h \left(1, \kappa^h \right)_{\Gamma^h}^h}{\left(1, 1 \right)_{\Gamma^h}^h} \right] \leq 0, \quad (3.16)$$

which leads to the desired perimeter decrease result (3.9) for $|\alpha| = 1$.

When $0 < |\alpha| \neq 1$, similar to the proof of theorem 1, to show $\frac{dL^h(t)}{dt} \leq 0$, we need the discrete version of power mean inequality [25][theorem 16]:

Lemma 2 (Power mean inequality, discrete) Suppose $n \in \mathbb{Z}^+$ and the non-zero parameters p, q satisfy $-\infty < p < q < \infty$. Let x_1, x_2, \dots, x_n be non-negative numbers if $p > 0$, or positive numbers if $p < 0$. For any $\omega_1, \omega_2, \dots, \omega_n$ satisfying $0 \leq \omega_i < +\infty \forall i$ with $\sum_{i=1}^n \omega_i > 0$, we have

$$\left(\frac{\sum_{i=1}^n \omega_i x_i^p}{\sum_{i=1}^n \omega_i} \right)^{\frac{1}{p}} \leq \left(\frac{\sum_{i=1}^n \omega_i x_i^q}{\sum_{i=1}^n \omega_i} \right)^{\frac{1}{q}}. \quad (3.17)$$

For the case $\alpha > 0, \alpha \neq 1$, we employ the discrete power mean inequality for $n = 2N, \omega_{2j-1} = \omega_{2j} = \frac{1}{2}|h_j|, x_{2j-1} = (\kappa^h)^\alpha(\rho_j^-), x_{2j} = (\kappa^h)^\alpha(\rho_{j-1}^+), \forall j = 1, 2, \dots, N, p = 1, q = \frac{\alpha+1}{\alpha}$, and $x_{2j-1} = (\kappa^h)(\rho_j^-), x_{2j} = (\kappa^h)(\rho_{j-1}^+), \forall j = 1, 2, \dots, N, p = 1, q = \alpha+1$, respectively, we obtain

$$\frac{\sum_{j=1}^N \frac{1}{2}|h_j| \left((\kappa^h)^\alpha(\rho_j^-) + (\kappa^h)^\alpha(\rho_{j-1}^+) \right)}{L^h(t)} \quad (3.18a)$$

$$\leq \left(\frac{\sum_{j=1}^N \frac{1}{2}|h_j| \left((\kappa^h)^{\alpha+1}(\rho_j^-) + (\kappa^h)^{\alpha+1}(\rho_{j-1}^+) \right)}{L^h(t)} \right)^{\frac{\alpha}{\alpha+1}},$$

$$\frac{\sum_{j=1}^N \frac{1}{2}|h_j| \left((\kappa^h)(\rho_j^-) + (\kappa^h)(\rho_{j-1}^+) \right)}{L^h(t)} \quad (3.18b)$$

$$\leq \left(\frac{\sum_{j=1}^N \frac{1}{2}|h_j| \left((\kappa^h)^{\alpha+1}(\rho_j^-) + (\kappa^h)^{\alpha+1}(\rho_{j-1}^+) \right)}{L^h(t)} \right)^{\frac{1}{\alpha+1}}.$$

Combining (3.18a) and (3.18b), we have

$$\begin{aligned} & \frac{1}{L^h(t)} ((\kappa^h)^\alpha, \kappa^h)_{\Gamma^h} \\ &= \left(\frac{\sum_{j=1}^N \frac{1}{2}|h_j| \left((\kappa^h)^{\alpha+1}(\rho_j^-) + (\kappa^h)^{\alpha+1}(\rho_{j-1}^+) \right)}{L^h(t)} \right) \\ &= \left(\frac{\sum_{j=1}^N \frac{1}{2}|h_j| \left((\kappa^h)^{\alpha+1}(\rho_j^-) + (\kappa^h)^{\alpha+1}(\rho_{j-1}^+) \right)}{L^h(t)} \right)^{\frac{\alpha}{\alpha+1}} \quad (3.19) \\ & \cdot \left(\frac{\sum_{j=1}^N \frac{1}{2}|h_j| \left((\kappa^h)^{\alpha+1}(\rho_j^-) + (\kappa^h)^{\alpha+1}(\rho_{j-1}^+) \right)}{L^h(t)} \right)^{\frac{1}{\alpha+1}} \end{aligned}$$

$$\begin{aligned}
&\geq \left(\frac{\sum_{j=1}^N \frac{1}{2} |h_j| \left((\kappa^h)^\alpha (\rho_j^-) + (\kappa^h)^\alpha (\rho_{j-1}^+) \right)}{L^h(t)} \right) \\
&\quad \cdot \left(\frac{\sum_{j=1}^N \frac{1}{2} |h_j| \left((\kappa^h) (\rho_j^-) + (\kappa^h) (\rho_{j-1}^+) \right)}{L^h(t)} \right) \\
&= \frac{1}{L^h(t)} \left((\kappa^h)^\alpha, 1 \right)_{\Gamma^h}^h \frac{1}{L^h(t)} (\kappa^h, 1)_{\Gamma^h}^h.
\end{aligned}$$

Similarly, for the case $\alpha < 0, \alpha \neq -1$, we employ the discrete power mean inequality for $n = 2N, \omega_{2j-1} = \omega_{2j} = \frac{1}{2} |h_j|, x_{2j-1} = (\kappa^h)^\alpha (\rho_j^-), x_{2j} = (\kappa^h)^\alpha (\rho_{j-1}^+), \forall j = 1, 2, \dots, N, p = \frac{\alpha+1}{\alpha}, q = 1$, and $x_{2j-1} = (\kappa^h) (\rho_j^-), x_{2j} = (\kappa^h) (\rho_{j-1}^+), \forall j = 1, 2, \dots, N, p = \alpha+1, q = 1$, respectively, we obtain

$$\left(\frac{\sum_{j=1}^N \frac{1}{2} |h_j| \left((\kappa^h)^{\alpha+1} (\rho_j^-) + (\kappa^h)^{\alpha+1} (\rho_{j-1}^+) \right)}{L^h(t)} \right)^{\frac{\alpha}{\alpha+1}} \quad (3.20a)$$

$$\leq \frac{\sum_{j=1}^N \frac{1}{2} |h_j| \left((\kappa^h)^\alpha (\rho_j^-) + (\kappa^h)^\alpha (\rho_{j-1}^+) \right)}{L^h(t)},$$

$$\left(\frac{\sum_{j=1}^N \frac{1}{2} |h_j| \left((\kappa^h)^{\alpha+1} (\rho_j^-) + (\kappa^h)^{\alpha+1} (\rho_{j-1}^+) \right)}{L^h(t)} \right)^{\frac{1}{\alpha+1}} \quad (3.20b)$$

$$\leq \frac{\sum_{j=1}^N \frac{1}{2} |h_j| \left((\kappa^h) (\rho_j^-) + (\kappa^h) (\rho_{j-1}^+) \right)}{L^h(t)}.$$

Using (3.20a) and (3.20b), by the same argument as (3.19), we have

$$\frac{1}{L^h(t)} \left((\kappa^h)^\alpha, \kappa^h \right)_{\Gamma^h}^h \leq \frac{1}{L^h(t)} \left((\kappa^h)^\alpha, 1 \right)_{\Gamma^h}^h \frac{1}{L^h(t)} (\kappa^h, 1)_{\Gamma^h}^h \quad (3.21)$$

Combining (3.13), (3.19), (3.21) and $\alpha\beta < 0$, we obtain

$$\frac{dL^h(t)}{dt} = \beta \left[\left((\kappa^h)^\alpha, \kappa^h \right)_{\Gamma^h}^h - \frac{\left((\kappa^h)^\alpha, 1 \right)_{\Gamma^h}^h \left(1, \kappa^h \right)_{\Gamma^h}^h}{\left(1, 1 \right)_{\Gamma^h}^h} \right] \leq 0, \quad (3.22)$$

which means that the desired perimeter decrease result (3.9) is also valid for $0 < |\alpha| \neq 1$. To sum up, the PFEM semi-discrete scheme (3.5) is energy decreasing for all α cases. The proof is completed.

4 A structure-preserving PFEM and its properties

4.1 A fully-discrete scheme

Let $\tau > 0$ be the time step size and $t_m = m\tau$ be the discrete time levels for $m \geq 0$. Assume that $\Gamma^m := X^m(\cdot) = (x^m(\cdot), y^m(\cdot))^T \in [\mathbb{V}^h]^2$ and $\kappa^m(\cdot) \in \mathbb{V}^h$ are the numerical approximations of $\Gamma^h(t_m) := X^h(\cdot, t_m)$ and $\kappa^h(\cdot, t_m)$, respectively, here $(X^h(\cdot, t), \kappa^h(\cdot, t)) \in [\mathbb{V}^h]^2 \times \mathbb{V}^h$ is the solution of the semi-discretization (3.5). Similarly, Γ^m is composed by segments $\{h_j^m\}_{j=1}^N$, which satisfies

$$\min_{1 \leq j \leq N} |h_j^m| > 0 \quad \text{with } h_j^m := X^m(\rho_j) - X^m(\rho_{j-1}), \quad \forall j = 1, 2, \dots, N, \quad (4.1)$$

and $\kappa^m(\cdot)$ satisfies the following assumption:

$$\kappa^m(\rho_j) \geq 0 \forall 0 < \alpha \neq 1 \quad \text{and} \quad \kappa^m(\rho_j) > 0 \forall \alpha < 0, \quad \forall j = 0, 1, \dots, N, \quad m \geq 0. \quad (4.2)$$

And the unit tangential vector τ^m and the outward unit normal vector n^m of the curve Γ^m are constant vectors on each interval I_j , which can be computed as

$$\tau^m|_{I_j} = \frac{h_j^m}{|h_j^m|} := \tau_j^m, \quad n^m|_{I_j} = -(\tau_j^m)^\perp = -\frac{(h_j^m)^\perp}{|h_j^m|} := n_j^m, \quad \forall j = 1, 2, \dots, N. \quad (4.3)$$

Then a structure-preserving parametric finite element fully discrete scheme (SP-PFEM) based on the backward Euler method in time and a proper approximation of the unit normal vector is constructed as: Given the initial curve $\Gamma^0 := \Gamma^h(0) \in [\mathbb{V}^h]^2$, find the closed curve $\Gamma^{m+1} := X^{m+1}(\cdot) = (x^{m+1}(\cdot), y^{m+1}(\cdot))^T \in [\mathbb{V}^h]^2$ and the mean curvature $\kappa^{m+1}(\cdot) \in \mathbb{V}^h$ for $m \geq 0$ such that

$$\begin{cases} \left(\frac{X^{m+1} - X^m}{\tau} \cdot n^{m+\frac{1}{2}}, \phi^h \right)_{\Gamma^m}^h - \left(\beta(\kappa^{m+1})\alpha - \lambda^{m+1}, \phi^h \right)_{\Gamma^m}^h = 0, & \phi^h \in \mathbb{V}^h, \\ \left(\kappa^{m+1} n^{m+\frac{1}{2}}, \omega^h \right)_{\Gamma^m}^h - \left(\partial_s X^{m+1}, \partial_s \omega^h \right)_{\Gamma^m}^h = 0, & \omega^h \in [\mathbb{V}^h]^2, \end{cases} \quad (4.4)$$

where

$$\lambda^{m+1} = \frac{(\beta(\kappa^{m+1})\alpha, 1)_{\Gamma^m}^h}{(1, 1)_{\Gamma^m}^h}, \quad (4.5)$$

and

$$n^{m+\frac{1}{2}} = -\frac{1}{2} (\partial_s X^m(s) + \partial_s X^{m+1}(s))^\perp = -\frac{(\partial_\rho X^m(\rho) + \partial_\rho X^{m+1}(\rho))^\perp}{2|\partial_\rho X^m(\rho)|}.$$

4.2 Area conservation and perimeter decrease

Let A^m be the total enclosed area and L^m be the perimeter of Γ^m , which can be written as

$$A^m = \frac{1}{2} \sum_{j=1}^N (x_j^m - x_{j-1}^m)(y_j^m + y_{j-1}^m), \quad L^m = \sum_{j=1}^N |h_j^m| = (1, 1)_{\Gamma^m}^h, \quad m \geq 0. \quad (4.6)$$

Then we can prove that the fully discrete scheme (4.4) preserves the two geometric structures.

Theorem 3 (Area conservation and perimeter decrease)

Let $(X^{m+1}(\cdot), \kappa^{m+1}(\cdot)) \in [\mathbb{V}^h]^2 \times \mathbb{V}^h$ be a solution of the proposed SP-PFEM (4.4) with the assumption (4.2) holds on $\kappa^{m+1}(\cdot)$. Then there holds

$$A^{m+1} = A^m \equiv A^0, \quad L^m \leq L^{m-1} \leq \dots \leq L^0, \quad (4.7)$$

i.e., the area is preserving and the perimeter is decreasing.

Proof By using a linear interpolation of X^{m+1} and X^m , we can introduce the approximate solution $\Gamma^h(\vartheta) = X^h(\rho, \vartheta)$ as

$$\Gamma^h(\vartheta) = (1 - \vartheta)X^m(\rho) + \vartheta X^{m+1}(\rho), \quad 0 \leq \rho \leq 1, \quad 0 \leq \vartheta \leq 1. \quad (4.8)$$

Let $B(\vartheta)$ be the area enclosed by $\Gamma^h(\vartheta)$. By applying theorem 2.1 in [7] and taking $\phi^h \equiv 1$ in (4.4), we obtain

$$\begin{aligned} B(1) - B(0) &= - \int_0^1 [X^{m+1} - X^m] \cdot \left[\frac{1}{2} \partial_\rho X^m(\rho) + \frac{1}{2} \partial_\rho X^{m+1}(\rho) \right]^\perp d\rho \\ &= \left((X^{m+1} - X^m) \cdot n^{m+\frac{1}{2}}, 1 \right)_{\Gamma^m}^h \\ &= \tau\beta \left[\left((\kappa^{m+1})^\alpha, 1 \right)_{\Gamma^m}^h - \frac{\left((\kappa^{m+1})^\alpha, 1 \right)_{\Gamma^m}^h (1, 1)_{\Gamma^m}^h}{(1, 1)_{\Gamma^m}^h} \right] \equiv 0, \end{aligned} \quad (4.9)$$

which implies $B(1) = B(0)$, i.e., $A^{m+1} = A^m$. Thus the first formula in (4.7) is true.

Now we aim to get the perimeter decrease property. Taking $\phi^h = \kappa^{m+1}$ and $\omega^h = X^{m+1} - X^m$ in (4.4), we can arrive at

$$\begin{aligned} (\partial_s X^{m+1}, \partial_s (X^{m+1} - X^m))_{\Gamma^m}^h &= \left(\kappa^{m+1} n^{m+\frac{1}{2}}, (X^{m+1} - X^m) \right)_{\Gamma^m}^h \\ &= \tau \left(\beta (\kappa^{m+1})^\alpha - \lambda^{m+1}, \kappa^{m+1} \right)_{\Gamma^m}^h \\ &= \tau\beta \left[\left((\kappa^{m+1})^\alpha, \kappa^{m+1} \right)_{\Gamma^m}^h - \frac{\left((\kappa^{m+1})^\alpha, 1 \right)_{\Gamma^m}^h (\kappa^{m+1}, 1)_{\Gamma^m}^h}{(1, 1)_{\Gamma^m}^h} \right]. \end{aligned} \quad (4.10)$$

By using a similar argument as the proof of the perimeter decrease part in theorem 2, we know that

$$\begin{aligned} & (\partial_s X^{m+1}, \partial_s (X^{m+1} - X^m))_{\Gamma^m}^h \\ &= \tau \beta \left[((\kappa^{m+1})^\alpha, \kappa^{m+1})_{\Gamma^m}^h - \frac{((\kappa^{m+1})^\alpha, 1)_{\Gamma^m}^h (\kappa^{m+1}, 1)_{\Gamma^m}^h}{(1, 1)_{\Gamma^m}^h} \right] \leq 0. \end{aligned} \quad (4.11)$$

On the other hand, since $u \cdot v \leq \frac{1}{2}(|u|^2 + |v|^2)$, $\forall u, v \in \mathbb{R}^2$, there holds

$$\begin{aligned} & (\partial_s X^{m+1}, \partial_s (X^{m+1} - X^m))_{\Gamma^m}^h \\ &= \sum_{j=1}^N |h_j^m| \frac{h_j^{m+1}}{|h_j^m|} \cdot \frac{h_j^{m+1} - h_j^m}{|h_j^m|} \\ &\geq \sum_{j=1}^N \frac{1}{2} \left(\left| \frac{h_j^{m+1}}{h_j^m} \right|^2 - 1 \right) |h_j^m| \geq \sum_{j=1}^N \left(\frac{|h_j^{m+1}|}{|h_j^m|} - 1 \right) |h_j^m| \\ &= \sum_{j=1}^N (|h_j^{m+1}| - |h_j^m|) = L^{m+1} - L^m. \end{aligned} \quad (4.12)$$

Then the desired second result in (4.7) follows from (4.11) and (4.12) immediately. Therefore, the fully-discrete scheme (4.4) is structure-preserving. The proof is completed.

4.3 The iterative solver

To solve the nonlinear system (4.4), the Newton's iterative method is adopted to derive $(X^{m+1}(\cdot), \kappa^{m+1}(\cdot)) \in [\mathbb{V}^h]^2 \times \mathbb{V}^h$. In the i -th iteration, given $(X^{m+1,i}(\cdot), \kappa^{m+1,i}(\cdot)) \in [\mathbb{V}^h]^2 \times \mathbb{V}^h$, for any $(\omega^h, \phi^h) \in [\mathbb{V}^h]^2 \times \mathbb{V}^h$, the Newton direction $(X^\delta(\cdot), \kappa^\delta(\cdot)) \in [\mathbb{V}^h]^2 \times \mathbb{V}^h$ can be obtained by

$$\begin{aligned} & \left(\frac{X^\delta}{\tau} \cdot n^{m+\frac{1}{2},i}, \phi^h \right)_{\Gamma^m}^h + \left(\frac{X^{m+1,i} - X^m}{\tau} \cdot \frac{(-\partial_\rho X^\delta)^\perp}{2|\partial_\rho X^m|}, \phi^h \right)_{\Gamma^m}^h \\ & - \alpha \beta \left((\kappa^{m+1,i})^{\alpha-1} \kappa^\delta, \phi^h \right)_{\Gamma^m}^h + \alpha \beta \left(\frac{((\kappa^{m+1,i})^{\alpha-1} \kappa^\delta, 1)_{\Gamma^m}^h}{(1, 1)_{\Gamma^m}^h}, \phi^h \right)_{\Gamma^m}^h \end{aligned} \quad (4.13a)$$

$$\begin{aligned} &= - \left(\frac{X^{m+1,i} - X^m}{\tau} \cdot n^{m+\frac{1}{2},i}, \phi^h \right)_{\Gamma^m}^h + \beta \left((\kappa^{m+1,i})^\alpha - \frac{((\kappa^{m+1,i})^\alpha, 1)_{\Gamma^m}^h}{(1, 1)_{\Gamma^m}^h}, \phi^h \right)_{\Gamma^m}^h, \\ & \left(\kappa^\delta n^{m+\frac{1}{2},i}, \omega^h \right)_{\Gamma^m}^h + \left(\kappa^{m+1,i} \frac{(-\partial_\rho X^\delta)^\perp}{2|\partial_\rho X^m|}, \omega^h \right)_{\Gamma^m}^h - \left(\partial_s X^\delta, \partial_s \omega^h \right)_{\Gamma^m}^h \\ &= - \left(\kappa^{m+1,i} n^{m+\frac{1}{2},i}, \omega^h \right)_{\Gamma^m}^h + \left(\partial_s X^{m+1,i}, \partial_s \omega^h \right)_{\Gamma^m}^h, \end{aligned} \quad (4.13b)$$

where

$$n^{m+\frac{1}{2},i} = -\frac{1}{2|\partial_\rho X^m|} (\partial_\rho X^m + \partial_\rho X^{m+1,i})^\perp.$$

For each $m \geq 0$, we set $X^{m+1,i+1} = X^{m+1,i} + X^\delta$, $\kappa^{m+1,i+1} = \kappa^{m+1,i} + \kappa^\delta$ and typically choose the initial guess $X^{m+1,0} = X^m$, $\kappa^{m+1,0} = \kappa^m$. Then we repeat the iteration (4.13a)–(4.13b) until

$$\max_{0 \leq j \leq N} (|X^{m+1,i+1}(\rho_j) - X^{m+1,i}(\rho_j)| + |\kappa^{m+1,i+1}(\rho_j) - \kappa^{m+1,i}(\rho_j)|) \leq tol,$$

where tol is the chosen tolerance.

The Picard iteration method can also be taken as an alternative solver. In the i -th iteration, given $\kappa^{m+1,i}(\cdot) \in \mathbb{V}^h$, for any $(\omega^h, \phi^h) \in [\mathbb{V}^h]^2 \times \mathbb{V}^h$, we seek $(X^{m+1,i+1}(\cdot), \kappa^{m+1,i+1}(\cdot)) \in [\mathbb{V}^h]^2 \times \mathbb{V}^h$ such that

$$\left(\frac{X^{m+1,i+1}}{\tau} \cdot n^{m+\frac{1}{2},i}, \phi^h \right)_{\Gamma^m} - \beta \left((\kappa^{m+1,i})^{\alpha-1} \kappa^{m+1,i+1}, \phi^h \right)_{\Gamma^m} \quad (4.14a)$$

$$+ \beta \left(\frac{((\kappa^{m+1,i})^{\alpha-1} \kappa^{m+1,i+1}, 1)_{\Gamma^m}}{(1, 1)_{\Gamma^m}}, \phi^h \right)_{\Gamma^m} = \left(\frac{X^m}{\tau} \cdot n^{m+\frac{1}{2},i}, \phi^h \right)_{\Gamma^m},$$

$$\left(\kappa^{m+1,i+1} n^{m+\frac{1}{2},i}, \omega^h \right)_{\Gamma^m} - \left(\partial_s X^{m+1,i+1}, \partial_s \omega^h \right)_{\Gamma^m} = 0. \quad (4.14b)$$

5 Numerical results

In this section, numerical experiments are carried out to verify the performance of the proposed SP-PFEM (4.4). We will investigate the convergent rates and area conservation, examine the perimeter decrease property and mesh quality, and simulate the morphological evolutions of closed curves.

In order to measure the numerical error between Γ^m and $\Gamma(t_m)$, we adopt the manifold distance defined in [48] as $M(\Gamma_1, \Gamma_2) = |(\Omega_1 \setminus \Omega_2) \cup (\Omega_2 \setminus \Omega_1)| = |\Omega_1| + |\Omega_2| - 2|\Omega_1 \cap \Omega_2|$, where Γ_1 and Γ_2 denote any two closed curves, Ω_1 and Ω_2 are the regions enclosed by Γ_1 and Γ_2 , respectively, and $|\Omega|$ denotes the area of Ω . Then the numerical error $e^h(t_m)$ is defined by

$$e^h(t) |_{t=t_m} := M(\Gamma^m, \Gamma(t=t_m)), \quad m \geq 0.$$

To further verify the properties of the proposed SP-PFEM (4.4), we introduce the relative area loss function $\frac{\Delta A^h(t)}{A^h(0)}$, the normalized perimeter function $\frac{W^h(t)}{W^h(0)}$ and the mesh ratio $R^h(t)$ as

$$\frac{\Delta A^h(t)}{A^h(0)} |_{t=t_m} := \frac{A^m - A^0}{A^0}, \quad \frac{W^h(t)}{W^h(0)} |_{t=t_m} := \frac{L^m}{L^0}, \quad R^h(t) |_{t=t_m} := \frac{h_{\max}^m}{h_{\min}^m},$$

where A^m and L^m have been given in (4.6), $h_{\max}^m = \max_{1 \leq j \leq N} |h_j^m|$, $h_{\min}^m = \min_{1 \leq j \leq N} |h_j^m|$, and $R^h(t)$ can be used to measure the mesh quality.

In the following numerical simulations, since formally the proposed SP-PFEM (4.4) is first-order accuracy in temporal direction and second-order accuracy in spatial direction, we can take the size parameters as $\tau = \mathcal{O}(h^2)$, e.g. $\tau = h^2$, except where noted. In view of the fact that the exact solution $\Gamma(t)$ is usually not available, we replace $\Gamma(t = t_m)$ with the numerical approximation based on very small size parameters $h = 2^{-8}$ and $\tau = 2^{-16}$. In addition, at each time step, the nonlinear system (4.4) is solved by the Newton's iteration method (4.13a)–(4.13b), where the tolerance is chosen as 10^{-12} .

5.1 Convergent rates, area conservation, perimeter decrease and mesh quality

In this subsection, the initial shape is taken as an ellipse curve given by $\frac{x^2}{3^2} + y^2 = 1$ and the parameter β in the area-conserved generalized mean curvature flow (1.1)–(1.2) is chosen as $|\beta| = 1$ satisfying $\alpha\beta < 0$.

Figure 1 plots the spatial convergence rates of the proposed SP-PFEM (4.4) at different times t for different parameters α and β . We find the order of convergence can reach about 2 in spatial discretization.

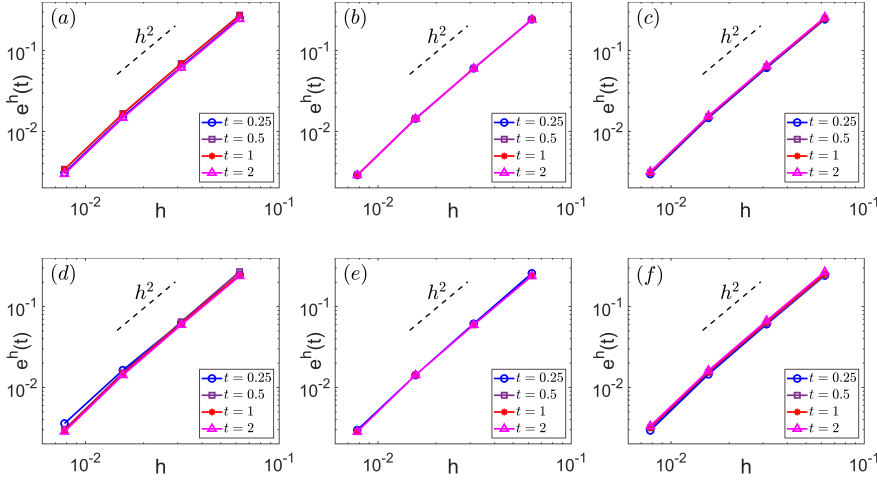


Fig. 1: Spatial convergence rates of the SP-PFEM (4.4) with $\tau = h^2$ at different times t for different parameters α and β : (a) $\alpha = 1, \beta = -1$; (b) $\alpha = 2, \beta = -1$; (c) $\alpha = 1/3, \beta = -1$; (d) $\alpha = -1, \beta = 1$; (e) $\alpha = -2, \beta = 1$; (f) $\alpha = -1/3, \beta = 1$.

Figure 2 shows the time evolutions of the relative area loss $\frac{\Delta A^h(t)}{A^h(0)}$ for different parameters α and β with fixed $h = 2^{-5}$ and $\tau = \frac{2}{25}h^2$, and depicts the iteration numbers of Newton's iterative (4.13a)–(4.13b) simultaneously. Numerical results confirm the area conservation property of the proposed SP-PFEM (4.4) in theorem 3 for the order of magnitude of the relative area loss is at around 10^{-15} , which is close

to the machine epsilon at around 10^{-16} . In addition, we observe that the number of Newton's iteration at each time step is around 1 to 3, which implies that it is efficient.

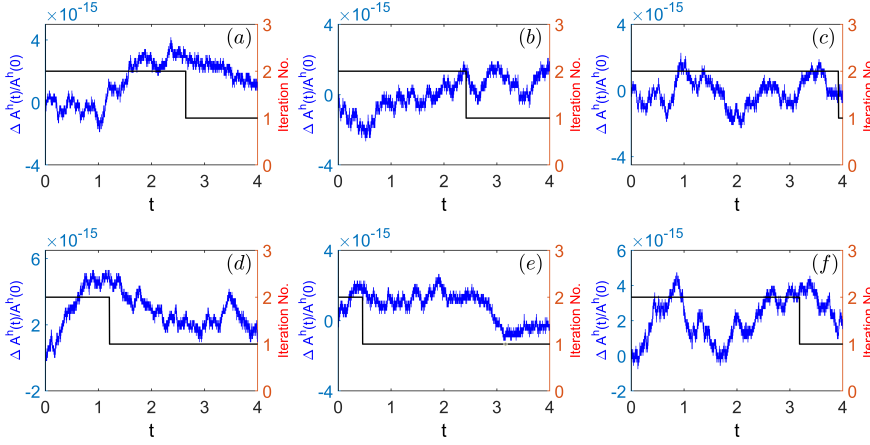


Fig. 2: Time evolutions of the normalized area loss $\frac{\Delta A^h(t)}{A^h(0)}$ (blue line) and iteration number (black line) of the SP-PFEM (4.4) for fixed $h = 2^{-5}$ and $\tau = \frac{2}{25}h^2$, where we choose the following parameters α and β : (a) $\alpha = 1, \beta = -1$; (b) $\alpha = 2, \beta = -1$; (c) $\alpha = 1/3, \beta = -1$; (d) $\alpha = -1, \beta = 1$; (e) $\alpha = -2, \beta = 1$; (f) $\alpha = -1/3, \beta = 1$.

To examine the unconditionally perimeter decrease, we show the normalized perimeter $\frac{W^h(t)}{W^h(0)}$ with fixed $h = 2^{-4}$ for different time step τ in Figure 3. It can be seen from Figure 3 that the normalized perimeter indeed decreases in time under different τ , which numerically substantiates the theoretical analysis in theorem 3.

Figure 4 depicts the time evolutions of the mesh ratio indicator $R^h(t)$ for different h . By using a uniform partition of the polar angle, the initial curve is discretized into a polygonal curve with non-uniform distribution with respect to the arc length. As time evolves, we can see the mesh ratio indicator $R^h(t)$ gradually decreases to approximate 1, which implies that the mesh points on the polygonal curve eventually be equally distributed, i.e., asymptotic equal mesh distribution. This property can follow from proposition 2.1 in [7].

5.2 Application of the SP-PFEM (4.4) for morphological evolutions

Here we will use the SP-PFEM (4.4) to simulate morphological evolutions of closed curves governed by the area-conserved generalized mean curvature flow (1.1)–(1.2). The evolutions of the initial ellipse curve $\frac{x^2}{32} + y^2 = 1$ for different parameters α and β are depicted in Figure 5. We observe that all curves evolve into a circle finally. Furthermore, when $\alpha = 1$ and $\beta = -1$, we apply the SP-PFEM (4.4)

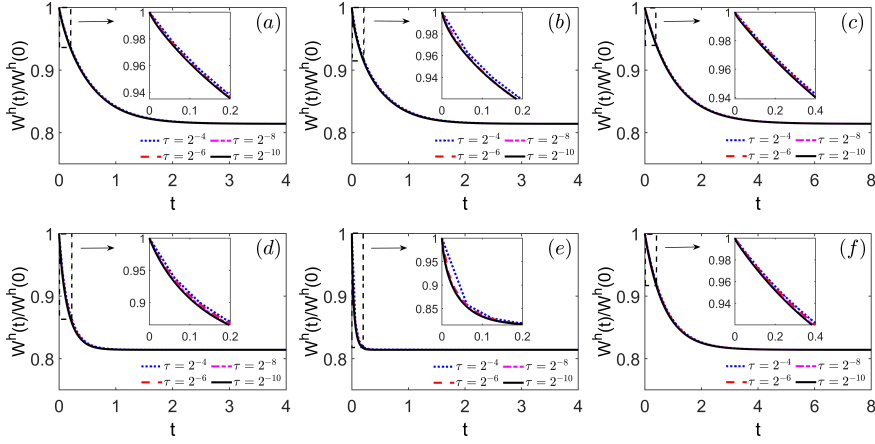


Fig. 3: Time evolutions of the normalized perimeter $\frac{W^h(t)}{W^h(0)}$ of the SP-PFEM (4.4) with fixed $h = 2^{-4}$ for different τ , where we choose the following parameters α and β : (a) $\alpha = 1, \beta = -1$; (b) $\alpha = 2, \beta = -1$; (c) $\alpha = 1/3, \beta = -1$; (d) $\alpha = -1, \beta = 1$; (e) $\alpha = -2, \beta = 1$; (f) $\alpha = -1/3, \beta = 1$.

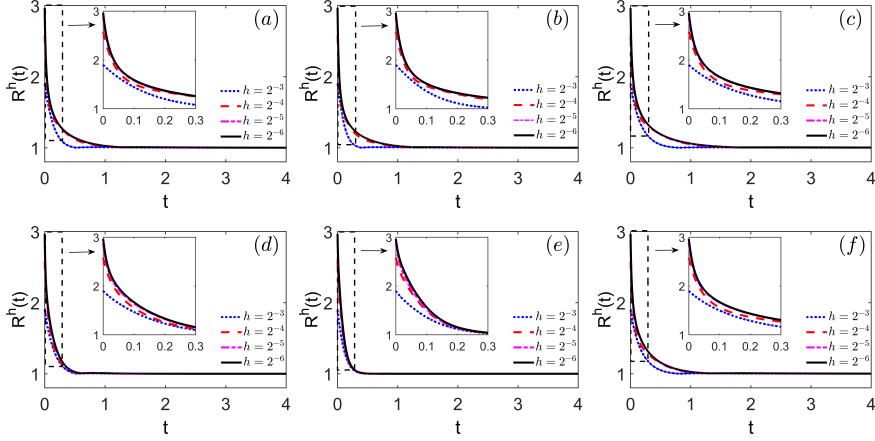


Fig. 4: Time evolutions of the mesh ratio $R^h(t)$ of the SP-PFEM (4.4) with $\tau = h^2$ for different h , where we choose the following parameters α and β : (a) $\alpha = 1, \beta = -1$; (b) $\alpha = 2, \beta = -1$; (c) $\alpha = 1/3, \beta = -1$; (d) $\alpha = -1, \beta = 1$; (e) $\alpha = -2, \beta = 1$; (f) $\alpha = -1/3, \beta = 1$.

to three more complex initial curves given by the following cases:

$$\text{(Case I): } x = (2 + \cos(6\theta)) \cos \theta, \quad y = (2 + \cos(6\theta)) \sin \theta,$$

$$\text{(Case II): } x = \cos \theta, \quad y = 2 \sin \theta - 1.9 \sin^3 \theta,$$

$$\text{(Case III): } x = \cos \theta, \quad y = \frac{1}{2} \sin \theta + \sin(\cos \theta) + (0.2 + \sin \theta \sin^2(3\theta)) \sin \theta,$$

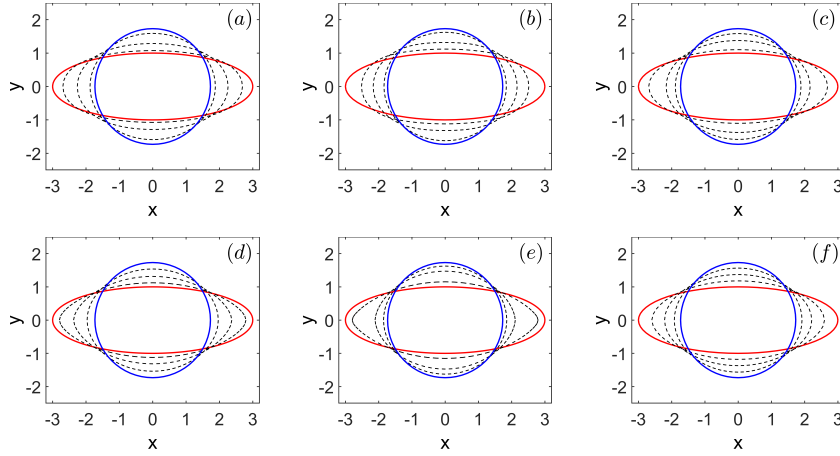


Fig. 5: Morphological evolutions of the initial ellipse curve (red solid line) towards its equilibrium shape (blue solid line) at different times (dashed lines) for different parameters α and β as follows: (a) $\alpha = 1$, $\beta = -1$, $t \in \{0.25, 0.75, 2\}$; (b) $\alpha = 2$, $\beta = -1$, $t \in \{0.25, 0.75, 2\}$; (c) $\alpha = 1/3$, $\beta = -1$, $t \in \{0.5, 2, 4\}$; (d) $\alpha = -1$, $\beta = 1$, $t \in \{0.05, 0.2, 0.5\}$; (e) $\alpha = -2$, $\beta = 1$, $t \in \{0.01, 0.1, 0.2\}$; (f) $\alpha = -1/3$, $\beta = 1$, $t \in \{0.5, 1.25, 2.5\}$. Here we choose $h = 2^{-6}$ and $\tau = h^2$.

where $\theta \in [0, 2\pi]$. Figure 6, Figure 7 and Figure 8 depict the curve evolutions of these initial shapes, respectively. It can be seen in Figure 6 that the six petals of the curve (Case I) gradually disappear and a circle is finally formed. Analogous numerical results for the complex curves (Case II) and (Case III) can be observed in Figure 7 and Figure 8, respectively. These numerical examples further demonstrate the applicability and reliability of the SP-PFEM (4.4).

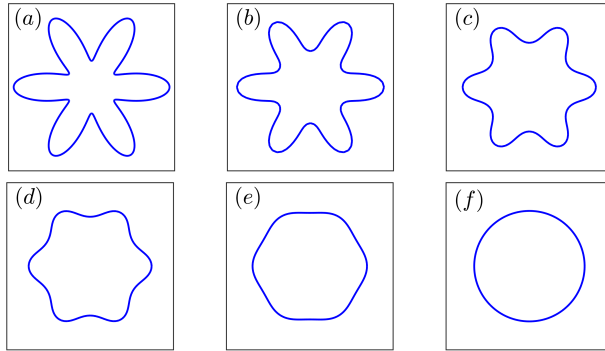


Fig. 6: Evolution of the initial curve (Case I) at different times: (a) $t = 0$, (b) $t = 0.05$, (c) $t = 0.15$, (d) $t = 0.25$, (e) $t = 0.4$, (f) $t = 1$. Parameters are chosen as $\alpha = 1$, $\beta = -1$, $h = 2^{-7}$ and $\tau = h^2$.

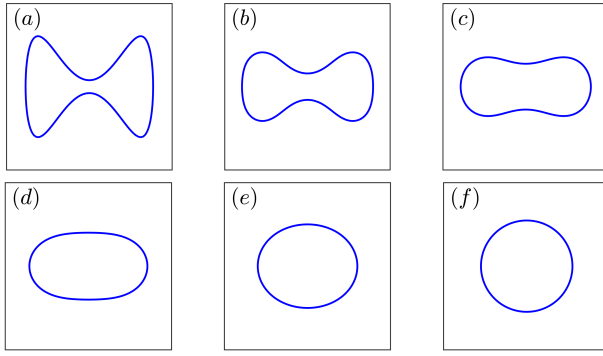


Fig. 7: Evolution of the initial curve (Case II) at different times: (a) $t = 0$, (b) $t = 0.05$, (c) $t = 0.1$, (d) $t = 0.2$, (e) $t = 0.4$, (f) $t = 1$. Parameters are chosen as $\alpha = 1$, $\beta = -1$, $h = 2^{-7}$ and $\tau = h^2$.

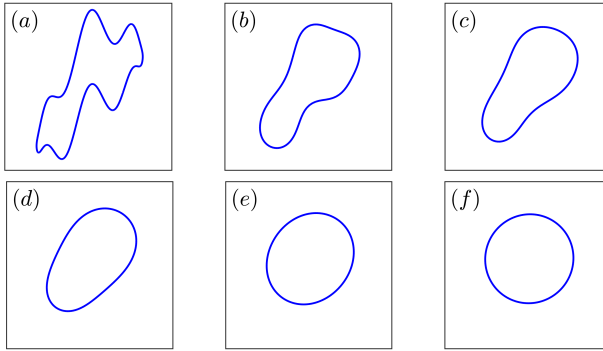


Fig. 8: Evolution of the initial curve (Case III) at different times: (a) $t = 0$, (b) $t = 0.05$, (c) $t = 0.1$, (d) $t = 0.2$, (e) $t = 0.5$, (f) $t = 1$. Parameters are chosen as $\alpha = 1$, $\beta = -1$, $h = 2^{-7}$ and $\tau = h^2$.

6 Conclusions

This study investigated numerical approximation of the area-conserved generalized mean curvature flow. We present a variational formulation and prove that it preserves two fundamental geometric structures of flows: the conservation of the area enclosed by the closed curve and the decrease of the perimeter of the curve. Then the variational problem is discretized in space by PFEM, and the structure-preserving property is also established for the semi-discrete scheme. Finally, a fully-discrete scheme is constructed by using the backward Euler method

in time and piecewise linear parametric finite element approximation in space. We prove that the proposed method preserves the two essential geometric structures simultaneously at the discrete level. In the end, numerical results confirm these conclusions and suggest that the proposed SP-PFEM is second-order accurate in space and enjoys asymptotic equal mesh distribution during the evolution. Therefore, our work provides a reliable and powerful tool for the simulation of area-conserved generalized mean curvature flow in 2D. In the future, we will further explore the extension of the new SP-PFEM for volume-preserving generalized mean curvature flow in three dimensions.

References

1. Andrews, B.: Evolving convex curves. *Calc. Var. Partial Differ. Equ.* **7**(4), 315–371 (1998). DOI <https://doi.org/10.1007/s005260050111>
2. Andrews, B., Wei, Y.: Volume preserving flow by powers of the k th mean curvature. *J. Differ. Geom.* **117**(2), 193–222 (2021). DOI <https://doi.org/10.4310/jdg/1612975015>
3. Bänsch, E., Morin, P., Nochetto, R.H.: A finite element method for surface diffusion: the parametric case. *J. Comput. Phys.* **203**(1), 321–343 (2005). DOI <https://doi.org/10.1016/j.jcp.2004.08.022>
4. Bao, W., Garcke, H., Nürnberg, R., Zhao, Q.: Volume-preserving parametric finite element methods for axisymmetric geometric evolution equations. *J. Comput. Phys.* **460**, 111180 (2022). DOI <https://doi.org/10.1016/j.jcp.2022.111180>
5. Bao, W., Jiang, W., Li, Y.: A symmetrized parametric finite element method for anisotropic surface diffusion of closed curves. *arXiv preprint arXiv:2112.00508* (2021)
6. Bao, W., Jiang, W., Wang, Y., Zhao, Q.: A parametric finite element method for solid-state dewetting problems with anisotropic surface energies. *J. Comput. Phys.* **330**, 380–400 (2017). DOI <https://doi.org/10.1016/j.jcp.2016.11.015>
7. Bao, W., Zhao, Q.: A structure-preserving parametric finite element method for surface diffusion. *SIAM J. Numer. Anal.* **59**(5), 2775–2799 (2021). DOI <https://doi.org/10.1137/21m1406751>
8. Barrett, J.W., Garcke, H., Nürnberg, R.: Numerical approximation of anisotropic geometric evolution equations in the plane. *IMA J. Numer. Anal.* **28**(2), 292–330 (2007). DOI <https://doi.org/10.1093/imanum/drm013>
9. Barrett, J.W., Garcke, H., Nürnberg, R.: On the variational approximation of combined second and fourth order geometric evolution equations. *SIAM J. Sci. Comput.* **29**(3), 1006–1041 (2007). DOI <https://doi.org/10.1137/060653974>
10. Barrett, J.W., Garcke, H., Nürnberg, R.: A parametric finite element method for fourth order geometric evolution equations. *J. Comput. Phys.* **222**(1), 441–467 (2007). DOI <https://doi.org/10.1016/j.jcp.2006.07.026>
11. Barrett, J.W., Garcke, H., Nürnberg, R.: Parametric approximation of willmore flow and related geometric evolution equations. *SIAM J. Sci. Comput.* **31**(1), 225–253 (2008). DOI <https://doi.org/10.1137/070700231>
12. Barrett, J.W., Garcke, H., Nürnberg, R.: Parametric finite element approximations of curvature-driven interface evolutions. In: *Handb. Numer. Anal.*, vol. 21, pp. 275–423. Elsevier (2020). DOI <https://doi.org/10.1016/bs.hna.2019.05.002>
13. Cabezas-Rivas, E., Sinestrari, C.: Volume-preserving flow by powers of the m th mean curvature. *Calc. Var. Partial Differ. Equ.* **38**(3), 441–469 (2010). DOI <https://doi.org/10.1007/s00526-009-0294-6>
14. Deckelnick, K., Dziuk, G.: On the approximation of the curve shortening flow. *Calc. Var. Appl. Comput.* **326**, 100–108 (1995)
15. Deckelnick, K., Dziuk, G., Elliott, C.M.: Computation of geometric partial differential equations and mean curvature flow. *Acta Numer.* **14**, 139–232 (2005). DOI <https://doi.org/10.1017/s0962492904000224>
16. Dittberner, F.: Curve flows with a global forcing term. *J. Geom. Anal.* **31**(8), 8414–8459 (2021). DOI <https://doi.org/10.1007/s12220-020-00600-1>
17. Dolcetta, I.C., Vita, S.F., March, R.: Area-preserving curve-shortening flows: from phase separation to image processing. *Interface Free Bound.* **4**(4), 325–343 (2002). DOI <https://doi.org/10.4171/ifb/64>

18. Dziuk, G.: An algorithm for evolutionary surfaces. *Numer. Math.* **58**(1), 603–611 (1990). DOI <https://doi.org/10.1007/bf01385643>
19. Escher, J., Simonett, G.: The volume preserving mean curvature flow near spheres. *Proc. Amer. Math. Soc.* **126**(9), 2789–2796 (1998). DOI <https://doi.org/10.1090/s0002-9939-98-04727-3>
20. Gage, M.: On an area-preserving evolution equation for plane curves. *Contemp. Math.* **51**(5), 51–62 (1986). DOI <https://doi.org/10.1090/conm/051/848933>
21. Gage, M., Hamilton, R.S.: The heat equation shrinking convex plane curves. *J. Differ. Geom.* **23**(1), 69–96 (1986). DOI <https://doi.org/10.4310/jdg/1214439902>
22. Gerhardt, C.: Non-scale-invariant inverse curvature flows in euclidean space. *Calc. Var. Partial Differ. Equ.* **49**(1), 471–489 (2014). DOI <https://doi.org/10.1007/s00526-012-0589-x>
23. Grayson, M.A.: The heat equation shrinks embedded plane curves to round points. *J. Differ. Geom.* **26**(2), 285–314 (1987). DOI <https://doi.org/10.4310/jdg/1214441371>
24. Guo, H., Sun, Z.: On a family of inverse curvature flows for closed convex plane curves. *Nonlinear Anal.-Real World Appl.* **50**, 1–7 (2019). DOI <https://doi.org/10.1016/j.nonrwa.2019.04.010>
25. Hardy, G., Littlewood, J., Pólya, G.: *Inequalities* (Cambridge University Press, 1934)
26. Huisken, G.: Flow by mean curvature of convex surfaces into spheres. *J. Differ. Geom.* **20**(1), 237–266 (1984). DOI <https://doi.org/10.4310/jdg/1214438998>
27. Huisken, G.: The volume preserving mean-curvature flow. *J. Reine Angew. Math.* **382**, 35–48 (1987). DOI <https://doi.org/10.1515/crll.1987.382.35>
28. Huisken, G., Ilmanen, T.: The inverse mean curvature flow and the riemannian penrose inequality. *J. Differ. Geom.* **59**(3), 353–437 (2001). DOI <https://doi.org/10.4310/jdg/1090349447>
29. Ilmanen, T.: Higher regularity of the inverse mean curvature flow. *J. Differ. Geom.* **80**(3), 433–451 (2008). DOI <https://doi.org/10.4310/jdg/1226090483>
30. Jiang, W., Li, B.: A perimeter-decreasing and area-conserving algorithm for surface diffusion flow of curves. *J. Comput. Phys.* **443**, 110531 (2021). DOI <https://doi.org/10.1016/j.jcp.2021.110531>
31. Kublik, C., Esedođlu, S., Fessler, J.A.: Algorithms for area preserving flows. *SIAM J. Sci. Comput.* **33**(5), 2382–2401 (2011). DOI <https://doi.org/10.1137/100815542>
32. Li, H.: The volume-preserving mean curvature flow in euclidean space. *Pacific J. Math.* **243**(2), 331–355 (2009). DOI <https://doi.org/10.2140/pjm.2009.243.331>
33. Li, Y., Bao, W.: An energy-stable parametric finite element method for anisotropic surface diffusion. *J. Comput. Phys.* **446**, 110658 (2021). DOI <https://doi.org/10.1016/j.jcp.2021.110658>
34. Lin, T.C., Poon, C.C., Tsai, D.H.: Expanding convex immersed closed plane curves. *Calc. Var. Partial Differ. Equ.* **34**(2), 153–178 (2009). DOI <https://doi.org/10.1007/s00526-008-0180-7>
35. M Elliott, C., Fritz, H.: On approximations of the curve shortening flow and of the mean curvature flow based on the deturck trick. *IMA J. Numer. Anal.* **37**(2), 543–603 (2017). DOI <https://doi.org/10.1093/imanum/drw020>
36. Ma, L., Cheng, L.: A non-local area preserving curve flow. *Geom. Dedic.* **171**(1), 231–247 (2014). DOI <https://doi.org/10.1007/s10711-013-9896-4>
37. Mayer, U.F.: A numerical scheme for moving boundary problems that are gradient flows for the area functional. *European J. Appl. Math.* **11**(1), 61–80 (2000). DOI <https://doi.org/10.1017/s0956792599003812>
38. Ruuth, S.J., Wetton, B.T.: A simple scheme for volume-preserving motion by mean curvature. *J. Sci. Comput.* **19**(1), 373–384 (2003)
39. Sapiro, G., Tannenbaum, A.: On affine plane curve evolution. *J. Funct. Anal.* **119**(1), 79–120 (1994). DOI <https://doi.org/10.1006/jfan.1994.1004>
40. Scheuer, J.: Pinching and asymptotical roundness for inverse curvature flows in euclidean space. *J. Geom. Anal.* **26**(3), 2265–2281 (2016). DOI <https://doi.org/10.1007/s12220-015-9627-1>
41. Schulze, F.: Evolution of convex hypersurfaces by powers of the mean curvature. *Math. Z.* **251**(4), 721–733 (2005). DOI <https://doi.org/10.1007/s00209-004-0721-5>
42. Schulze, F.: Nonlinear evolution by mean curvature and isoperimetric inequalities. *J. Differ. Geom.* **79**(2), 197–241 (2008). DOI <https://doi.org/10.4310/jdg/1211512640>
43. Sevcovic, D., Mikula, K.: Evolution of plane curves driven by a nonlinear function of curvature and anisotropy. *SIAM J. Appl. Math.* **61**(5), 1473–1501 (2001). DOI <https://doi.org/10.1137/s0036139999359288>
44. Sinestrari, C.: Convex hypersurfaces evolving by volume preserving curvature flows. *Calc. Var. Partial Differ. Equ.* **54**(2), 1985–1993 (2015). DOI <https://doi.org/10.1007/s00526-015-0852-z>
45. Tsai, D.H., Wang, X.L.: On length-preserving and area-preserving nonlocal flow of convex closed plane curves. *Calc. Var. Partial Differ. Equ.* **54**(4), 3603–3622 (2015). DOI <https://doi.org/10.1007/s00526-015-0915-1>

46. Urbas, J.I.: An expansion of convex hypersurfaces. *J. Differ. Geom.* **33**(1), 91–125 (1991). DOI <https://doi.org/10.4310/jdg/1214446031>
47. Ushijima, T.K., Yazaki, S.: Convergence of a crystalline approximation for an area-preserving motion. *J. Comput. Appl. Math.* **166**(2), 427–452 (2004). DOI <https://doi.org/10.1016/j.cam.2003.08.041>
48. Zhao, Q., Jiang, W., Bao, W.: An energy-stable parametric finite element method for simulating solid-state dewetting. *IMA J. Numer. Anal.* **41**(3), 2026–2055 (2021). DOI <https://doi.org/10.1093/imanum/draa070>

Statements and Declarations

Funding

This research was supported by National Natural Science Foundation of China (Grant No. [11701523]).

Competing Interests

The authors have no relevant financial or non-financial interests to disclose.

Author Contributions

All authors contributed to the study conception and design.

Lifang Pei: Paper writing, Theoretical analysis, Numerical tests.

Yifei Li: Theoretical analysis, Writing-review and editing.

All authors read and approved the final manuscript.

Data Availability

The data generated or analyzed during the current study are available from the corresponding author on reasonable request.